Reinforcement of GFRP Tensile Specimens with Central Holes Using Bonded Composite Patches

Fernando E.L. Paiva, João M.L. Reis and Heraldo S. da Costa Mattos[*]

Laboratory of Theoretical and Applied Mechanics, Graduate Program in Mechanical Engineering, Federal Fluminense University, Rua Passo da Pátria 156, 24210-240, Niterói, RJ, Brazil

Abstract: The use of bonded composite patches is a promising repair/reinforcement method to extend service live of damaged structures. These patches are non-corroding, lightweight, easy to fabricate and have high specific modulus and strength. In this work, the tensile behavior of a patch-reinforced composite specimen with a central hole is analyzed experimentally. A 10-ply composite tensile specimen is prepared by using bidirectional woven e-glass fabric and epoxy resin as the matrix material. The damage is created in the specimen by drilling three different holes with 3, 6 and 10 mm diameter at the center. The specimen is then reinforced by bonding composite patches or carbon steel patches with different lengths as external patches on both external surfaces. Tensile tests have been carried out on the undamaged, damaged, and repaired specimens. From the tensile tests, it was possible to verify the reduction of the strength (measured by the rupture force) of the specimens with holes of 3 mm, 6 mm and 10 mm. The patches were manufactured using the same glass fiber reinforced plastic, GFRP, used in the specimens or carbon steel. The patches were 25,0 mm wide, 2,5 mm thick. The length was 20 mm, 40 mm or 60 mm. It was found that GFRP patches has better efficiency than carbon steel patches. The repairs with GFRP patches were able to restore between 80% and 90% of the mechanical properties of the intact GFRP specimen without the necessity to replace the composite material.

Keywords: GFRP tensile specimens, Damage, Composite reinforcement, Bonded Patches, Tensile tests, Delamination.

INTRODUCTION

Fiber-reinforced polymer composites are often used to repair damaged structures. The most common application nowadays, particularly in the oil and gas industries, is the repair of metal pipelines transporting liquids with localized corrosion damage that impairs its operation [1-4]. These systems can be subjected to pressure transients [5]

Such systems can be used for part-wall defects [6-9] but are also being used to repair through-wall defects, were, in addition to structural repair, leak prevention is very important [10-13]. Information on requirements and recommendations for qualification, design, installation, testing and inspection for the external application of composite repairs to corroded or damaged piping in the petroleum, petrochemical and natural gas industries can be found in standards, for example, the ISO 24817 [14] and ASME PCC-2 [15] standards.

Bonded patches can also be used to extend the life of metal components [16, 17]. In this case, patch size and bonding properties are very important. The main difficulty is to define the appropriate area and thickness

of the composite to guarantee a satisfactory level of structural integrity. It is important to highlight that the traditional standards for corroded pipelines [14, 15] only deal with the design of composite gloves and not bonded patches.

The repair of different kinds of damages in composite or metal structures using patches is still a subject of research. Fiber-reinforced polymer composites are being used, for instance, to repair cracks in laminates in aerospace industry and in civil engineering [17, 18].

The main goal of the present study is to compare the efficiency of the repair of glass fiber reinforced plastic ,GFRP, tensile specimens with central holes with diameters of 3 mm, 6 mm or 10 mm reinforced using GFRP patches with length of 20 mm, 40 mm or 60 mm. The ASTM D3039 [19] tensile test was used to measure the force and elongation required to rupture the specimen with the repair. The specimens were placed a safe distance from the handles of a universal testing machine and pulled until they fail. The increase in nominal stresses at the roots of the notches contributes severely to the increase in failure mechanisms due to brittle fracture. The stress concentration factor (Kt) is the ratio between the maximum stress at the root of the defect notch and the nominal stress that would act at the location if there were no notch. Thus, the higher the Kt, the greater the tension at the notch location.

*Address correspondence to this author at the Laboratory of Theoretical and Applied Mechanics, Graduate Program in Mechanical Engineering, Federal Fluminense University, Rua Passo da Pátria 156, 24210-240, Niterói, RJ, Brazil; Tel/Fax: + 55 21 991267672; E-mail: heraldomattos@id.uff.br

The application of composite materials in the most diverse industries has increased significantly. The GFRP was chosen due its application in an extensive array of markets such as aerospace and automotive industries. GFRP consists of a combination of glass fibers and polymeric resin, which are incorporated during the manufacturing process to impart mechanical and structural properties to the material. Another important advantage is the corrosion resistance offered by glass fibers. Unlike metals, which can corrode or rust in certain environments, GFRP is highly resistant to chemical attack and corrosion, making it a suitable choice for applications involving chemicals or harsh environments.

For this study, an important aspect taken into consideration was the manufacture of the GFRP test specimens using hand lay-up technique and drilling. The manual lamination process was the process used to manufacture the specimens. The process consists of applying resin to the fiber manually. Generally, curing is done at room temperature. It is the simplest and cheapest process. A layer of resin is applied to the mold. Then, the fiber is placed over the first layer. More resin and more layers of fiber are applied successively until the number of layers is reached. With the help of a brush, the resin is spread and, using a metal roller, the resin permeates the fiber. Depending on the viscosity of the resin, the manual work may be greater or lesser.

Preferably, the repair of composite materials should be carried out with the same material as the object to be repaired. Sometimes it is not possible, mainly due to the location where the repair is carried out. In addition to atmospheric conditions not being favorable to the curing process, it is often not possible to use the equipment and tools used in manufacturing. In these circumstances, it is acceptable to perform the repair using another technique. When carrying out the repair, the types of fibers used, the fiber orientations, the number of layers, the matrix resin, the geometry of the damage and the qualification of the repair procedure must be taken into consideration. The geometry of the defect is an important aspect. Defects in composites, during applications, have complex geometries and high stress concentrators [20]. Many of these defects have never been studied. A defect with complex geometry can easily be replaced by a hole that has already been studied.

In this scenario, the adhesive joint repair is being used to restore as much as possible the mechanical properties of the repaired equipment, piping, structure, or component to allow operational without accidents and unscheduled shutdowns. Adhesive joints will transfer loads more efficiently than bolted joints. In an adhesive joint, the entire adhesive area transfers tension between the joined materials, while in a bolted joint, the greatest tension is in the region around the bolt. Normally, many bolts are necessary to withstand the forces and tensions to which the material is being subjected. For each bolt it is necessary to drill a hole, which ends up weakening the material. In addition to introducing new stress concentrators, bolts can also corrode without proper preservation.

The efficiency of adhesive repair depends on patch dimensions, surface preparation, adhesive properties, adhesive thickness, curing time and temperature. If some of these factors are not fully met, the application of the adhesive will not be efficient [21]. The repairs of specimens using an adhesive need to consider the adhesion of the adhesives to the material substrates so that there is no detachment between the interfaces during loading applications. In addition to physical and chemical bonds, another important aspect is the anchoring of the adhesive in pores, cavities, and surface irregularities.

Surface treatment is not only to remove impurities, but also to create irregularities and increase roughness on the surface of the substrate to anchor the adhesive. The larger the contact area between adhesive and substrate, the larger the anchoring region will be, thus increasing the resistance to detachment of the adhesive caused by loads subjected to this interface. The thickness of the adhesive is another factor that can cause rapid separation of the patch from the repaired component due to low transfer between the patch and the adhesive. Several studies observed that the patch detachments begin at the ends of the patch width and in the center region of the hole. The propagation area increases until the patch completely detaches.

The application of such kind of reinforcement does not require a lot of training, however, lack of care during application can result in low resin, fiber breakage, fiber disorientation or delamination between layers. In this process, the amount of resin and ambient temperature are important variables. Ambient temperature is decisive in both handling and curing of the composite as it changes the viscosity of the resin. If the manufacturer's procedure for applying the resin is not correctly followed, there will be a reduction in the mechanical properties of the composite.

The defects are only visible when they occur close to the surface of the material and can be identified

using a flashlight. To detect defects and their extensions in the other layers, it is necessary to employ non-destructive testing such as thermography. Delamination is the most common type of damage and consists of the separation of one or more layers of fiber in the matrix. Voids are also common due the lack of resin. Several measures were taken to avoid these types of defects during the manufacture of the specimens and patches. Only visual inspection was carried out at the present work. The use of other non-destructive techniques will be addressed in future studies.

MATERIALS AND METHODS

Tables **1** and **2** show the properties of the woven fiberglass WR-326 from TEXIGLASS[®,] epoxy resin MC 109 and hardener FD 131 from EPOXYFIBER[®] used to manufacture the GFRP test specimens and GFRP patches. Table **3** shows the properties of the HUNTSMAN[®] Rengel SW 404 adhesive used to carry out the repairs.

Table 1:   Properties of the Fiber Glass wovenWR-326

Properties of The Fiber Glass WOV WR-326	
Grammage (g/m²)	326
Witdh (cm)	130
Linear Meter Per Roll (m)	100
Square Meter Per Roll (m²)	130
Thickness (mm)	0,3
Breaking Load (kgf/cm)	81,6
Type of Weaving	Canvas
Fiber Orientation	Bidirecional (0°/90°)

Table 2:   Properties of the Epoxy Resin MC 109

Properties of the Epoxy Resins	
Viscosity 25°C (cP)	12000 – 13000
Density (kg/m³)	1 160
Temperature of Heat Distortion (°C)	50
Young´S Modulus (GPa)	2,4 – 5,0
Bending Resistance (MPa)	60
Rupture Resistance (MPa)	73
Glass Transition Temperature (°C)	70
Cure Time (h)	24
Cure Temperature (°C)	60

Table 3:   Properties of Rengel SW 404 Adhesive

Propriedades Adesivo Rengel SW 404	
Young´S Modulus (kgf/mm²)	900 - 1000
Rupture Resistance (kgf/mm²)	5,0 – 6,0
Pressure Resistance (kgf/mm²)	13,0 – 15,0
Bending Resistance (kgf/mm²)	12,0 – 14,0
Impact Resistance (kgf/mm²)	7,5 - 9,5
Density (g/cm³)	1,8 - 1,9

The Figure **1** is a flow diagram of all steps before and after the tensile test according to ASTM 3039D.

The plates used to manufacture the GRFP specimens and GRFP patches were manufactured using hand lay-up lamination technique by stacking 10 layers of woven fiberglass in the same orientation. The first step was cut the woven fiberglass and to visually
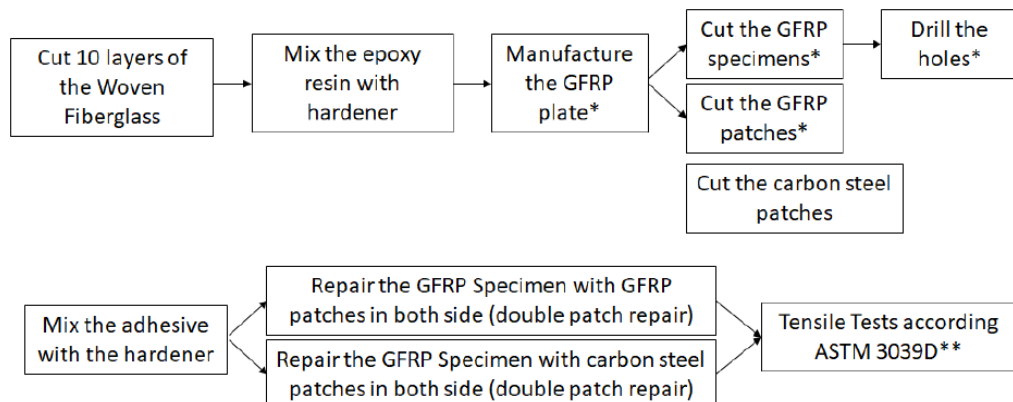
*visual inspection before the tensile test
**visual inspection after the tensile test

Figure 1: Flow Diagram.

inspect all the 10 layers to check if there were any broken fibers, ripples or wrinkles.

The epoxy resin and hardener were mixed with 10:1 proportion. Using a metal roller and brush, the resin was applied to the first layer of textile. The layer was visually inspected to detect areas with low resin permeation. If areas with low resin were found, new applications were made with the brush and then the roller was used. The second layer was stacked on top of the first layer. More resin was applied, and this process continued until all ten layers were stacked.

Figure 2: Press used to manufacture the GFRP plate.

There are three important aspects of the manual lamination process that need to be highlighted. The first concerns the orientations of the layers. Every time a new layer was applied over another, care was taken to ensure that the fibers were in the same orientation. All 10 layers need to be in the same orientation. The second deals with the resin application sequence. The resin must be applied with a brush. The metal roller

should only be used after applying the resin. The third point is about the force applied by the roller. The applicator must be careful not to overdo it and damage the fibers. Figure **2** shows the press used to manufacture the GFRP plate. The stacking was done between two metal plates and TECGLAZE® wax base was used as a release agent. The stack was placed in a press to ensure the specimens were 2.5 mm thick.

The plates were only demolded after 7 days of curing at room temperature. There was no difficulty in removing the mold as wax was applied. The plates were again visually inspected for defects. No delamination or lack of resin were detected in the surface layers. Figure **3** shows the plate after a 7 days cure.

Figure 3: GFRP plate after 7 days cure.

The cuts of the specimens and patches were made with a table saw. After cuts, the specimens and patches were visually inspected to check for delamination, fiber breakage or damage to the matrix caused by the saw. The specimens were measured
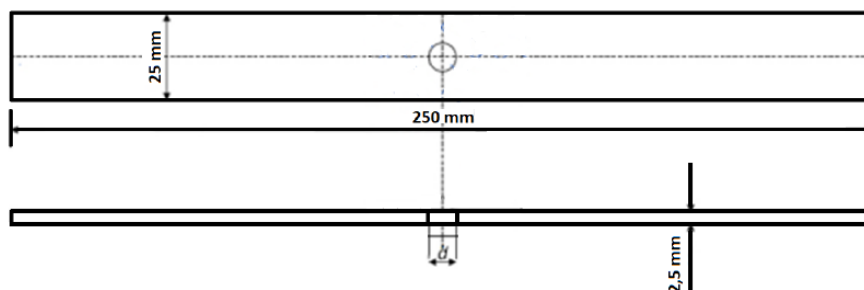
Figure 4: GFRP specimen dimensions.

Figure 5: Bench saw and bench drill.

after cutting with a caliper to ensure they were manufactured according to ASTM D3039. The GFRP patches were also measured to ensure they were manufactured according to specifications. The GFRP specimen dimensions are presented in Figure **4**.

The holes in the specimens were made with a bench drill shown in Figure **5**. A piece of wood was used to avoid delamination at the end of drilling for each specimen. Once again, all specimens were visually inspected, and no defects were identified.

The specimens drilled with 3 mm, 6 mm and 10 mm holes are shown in Figure **6**.

After the drilling, the repairs were made using the adhesive (Figure **6** and **7**). The GFRP patches were manufactured from the same plates used to

Figure 6: Specimens with 3 mm, 6 mm and 10 mm holes.
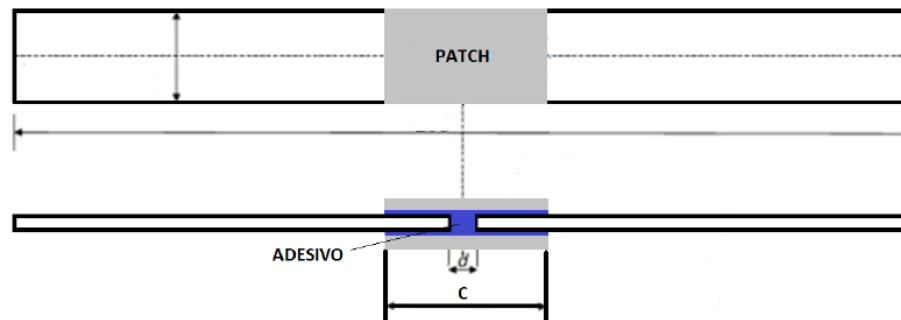
Figure 7: Adhesive repair using carbon steel patches and GFRP patches.

manufacture the specimens. The carbon steel patches were manufactured using a carbon steel plate. Only the carbon steel patches had surface treatment. The centers of the patches were positioned in the centers of the specimens. No surface treatments or roughness measurements were made on the specimens or patches.

The adhesive mixing and patch applications were done completely manually as shown in Figure **7**.

Figure 8: Mixture of adhesive and hardener.

The holes were filled with adhesives for later patch application. The patches were pressed so that there was better adhesion and anchoring of the adhesive (Figure **8**).

Figure 10: GFRP specimens after adhesive application and before cure.

Figure **9** shows the GFRP specimens after adhesive application and before cure. After curing for 7 days (Figure **10**), the average thickness of the films was 0.37
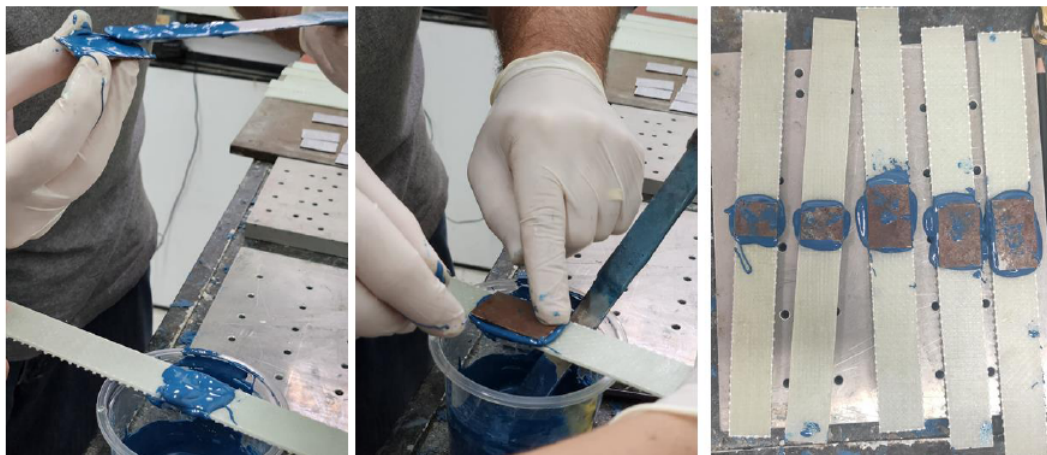
Figure 9: Carbon steel patches application.

mm. The excess of adhesive from the sides of the specimens were removed.
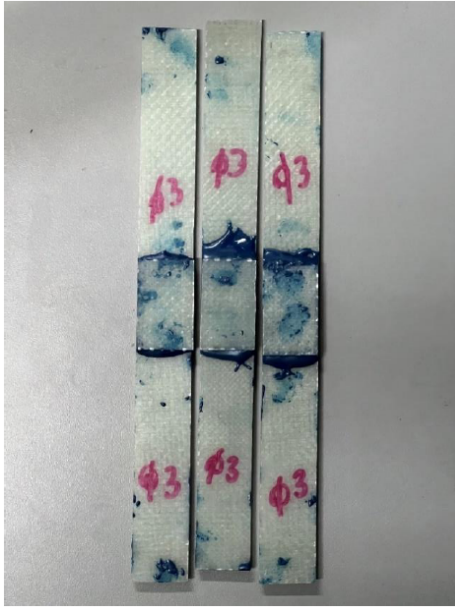
Figure 11: GFRP Specimens with GRFP patches ready for test.

Finally, the specimens were identified to begin the tensile tests. Tests 1, 2 and 3 are the testes of specimens without defect and repair. Table **4** shows the quantity of tests and the characteristics of each one.

The tensile tests followed the ASTM D3039 standard, which establishes the parameters and requirements for tests with composites. The equipment used to carry out the tests was the SHIMADZU® model AG-X machine. To position the specimen, the machine's standard clamps were used to clamp the ends of the specimens. The distance between the claws was 160 mm (Figure **11**).

RESULTS AND DISCUSSION

Table **5** presents the stress and strain at the rupture of all tests mentioned in Table **4**.

Table **5** contains the tensions and deformations at the rupture of all tests mentioned in Table **4**. The percentual of mechanical properties restored was calculated dividing the value of the rupture tension of

Table 4:   Tensile Test Matrix

Test	Hole Diameter (mm)	Patch Length (mm)	Patch Material
1, 2 and 3	-	-	-
4, 5 and 6	3	-	-
7, 8 and 9	3	20	GFRP
10, 11and 12	3	40	
13, 14 and 15	3	60	
16, 17 and 18	6	-	-
19, 20 and 21	6	20	GFRP
22, 23 and 24	6	40	
25, 26 and 27	6	60	
28, 29 and 30	10	-	-
31, 32 and 33	10	20	GFRP
34, 35 and 36	10	40	
37, 38 and 39	10	60	
40, 41 and 42	3	20	Carbon Steel
43, 44 and 45	3	40	
46, 47 and 48	3	60	
49, 50 and 51	6	20	
52, 53 and 54	6	40	
55, 56 and 57	6	60	
58, 59 and 60	10	20	
61, 62 and 63	10	40	
64, 65 and 66	10	60	

Table 5:   **Stress and Strain at Rupture of the Intact, Damaged, and Repaired Specimens with GFRP and Carbon Steel Patches (Average ± St. Dev)**

Test	Maximum Stress (MPa)	Strain (mm/mm)	Patch Material
1. 2 and 3	461.11 ± 7.42-	0.035 ±0.003	-
4. 5 and 6	374.21 ± 14.19	0.024 ±0.0006	-
7. 8 and 9	395.39 ± 11.13	0.024 ± 0.0015	GFRP
10. 11and 12	396.53 ± 15.56	0.023 ± 0.0006	
13. 14 and 15	408. 34 ± 7.00	0.041 ± 0.0006	
16. 17 and 18	277.67 ± 7.20	0.016 ± 0.0005	-
19. 20 and 21	353.81 ± 3.62	0.018 ± 0.0001	GFRP
22. 23 and 24	372.50 ± 13.63	0.019 ± 0.0002	
25. 26 and 27	361.43 ± 24.67	0.031 ± 0.0021	
28. 29 and 30	209.07 ± 29.83	0.014 ± 0.0026	-
31. 32 and 33	331.97 ± 9.41	0.016 ± 0.0006	GFRP
34. 35 and 36	349.93 ± 4.68	0.017 ± 0.0001	
37. 38 and 39	367.19 ± 5.25	0.027 ± 0.0017	
40. 41 and 42	358.63 ± 29.79	0.020 ± 0.0017	Carbon Steel
43. 44 and 45	364.27 ± 31.01	0.020 ± 0.0006	
46. 47 and 48	327.83 ± 16.88	0.019 ± 0.0012	
49. 50 and 51	306.10 ± 24.16	0.018 ± 0.0010	
52. 53 and 54	256.90 ± 25.72	0.016 ± 0.0006	
55. 56 and 57	286.07 ± 9.42	0.017 ± 0.0001	
58. 59 and 60	220.73 ± 22.34	0.014 ± 0.0005	
61. 62 and 63	243.47 ± 9.99	0.014 ± 0.0001	
64. 65 and 66	219.10 ± 1.73	0.013 ± 0.0001	

the specimen with repair with the rupture tension of the test 1 (468,54 MPa, see Table **6**). The test 1 value was chosen because it´s the highest value. The efficiency of the repair was calculated subtracting the lowest value of the damaged specimen from the value of the rupture tension of the specimen with the repair and dividing the result with the lowest value of the damaged specimen. The lowest value of the specimen with hole of 3 mm is test 5 (361,10 MPa), with hole of 6 mm is test 18 (269,40 MPa) and with hole of 10 mm is test 29 (175,00 MPa).

The tests with negative values of efficiency are not considered (taken as outliers). So, the results are: (i) For hole with 3 mm diameter and patches with 20 mm length, the best result is test 9 (406,58 MPa). The repair with GFRP restores more mechanical proprieties and is more efficient than the higher repair with carbon steel (test 42); (ii) For hole with 3 mm diameter and with patches with 40 mm length, the best result is test 12 (413,46 MPa). The repair with GFRP restores more mechanical proprieties and is more efficient than the

higher repair with carbon steel (test 43); (iii) For hole with 3 mm diameter and with patches with 60 mm length, the best result is test 15 (412,68 MPa). The repair with GFRP restores more mechanical proprieties and is more efficient than the higher repair with carbon steel (test 48); (iv) For hole with 6 mm diameter and patches with 20 mm length, the best result is test 20 (357,98 MPa). The repair with GFRP restores more mechanical proprieties and is more efficient than the higher repair with carbon steel (test 49); (v) For hole with 6 mm diameter and with patches with 40 mm length, the best result is test 24 (383,04 MPa). The repair with GFRP restores more mechanical proprieties and is more efficient than the higher repair with carbon steel (test 52); (vi) For hole with 6 mm diameter and patches with 60 mm length, the best result is test 25 (377,30 MPa). The repair with GFRP restores more mechanical proprieties and is more efficient than the higher repair with carbon steel (test 57); (vii) For hole with 10 mm diameter and patches and with 20 mm length, the best result is test 38 (338,73 MPa). The repair with GFRP restores more mechanical proprieties

Table 6:   Percentual of Mechanical Proprieties Restored and Efficiency of the Reinforced Specimens

Test	Restore (%)	Efficiency (%)	Test	Restore (%)	Eficiency (%)
7	82,05%	6,46%	40	73,44%	-4,71%
8	84,32%	9,40%	41	72,33%	-6,15%
9	86,80%	12,62%	42	83,86%	8,81%
10	81,72%	6,03%	43	83,81%	8,75%
11	83,93%	8,90%	44	70,69%	-8,28%
12	88,24%	14,50%	45	78,73%	2,16%
13	87,95%	14,12%	46	65,86%	-14,54%
14	85,43%	10,85%	47	71,43%	-7,31%
15	88,08%	14,28%	48	72,61%	-5,79%
19	75,02%	30,48%	49	68,34%	18,86%
20	76,40%	32,88%	50	59,38%	3,27%
21	75,11%	30,64%	51	68,28%	18,75%
22	76,22%	32,56%	52	58,44%	1,63%
23	80,54%	40,07%	53	57,54%	0,07%
24	81,75%	42,18%	54	48,51%	-15,63%
25	80,53%	40,05%	55	60,23%	4,75%
26	79,82%	38,82%	56	59,59%	3,64%
27	71,07%	23,61%	57	63,35%	10,17%
31	71,71%	91,98%	58	52,59%	40,80%
32	72,29%	93,56%	59	44,84%	20,06%
33	68,56%	83,55%	60	43,90%	17,54%
34	73,96%	98,02%	61	54,40%	45,66%
35	74,27%	98,85%	62	51,03%	36,63%
36	75,82%	103,01%	63	50,45%	35,09%
37	77,13%	106,50%	64	46,68%	24,97%
38	78,67%	110,62%	65	46,44%	24,34%
39	79,31%	112,34%	66	47,17%	26,29%

and is more efficient than the higher repair with carbon steel (test 58); (viii) For hole with 10 mm diameter and with patches with 40 mm length, the best result is test 12 (355,26 MPa). The repair with GFRP restores more mechanical proprieties and is more efficient than the higher repair with carbon steel (test 61). (ix) For hole with 10 mm diameter and with patches with 60 mm length, the best result is test 39 (371,60 MPa). The repair with GFRP restores more mechanical proprieties and is more efficient than the higher repair with carbon steel (test 66).

The higher results for holes with 3 mm and 6 mm diameters are the GFRP patch with 40 mm of length. The higher result for hole with 10 mm is the repair with a GFRP patch with 60 mm of length. Figures **12**, **13** and **14** present typical stress strain curves for different situations.
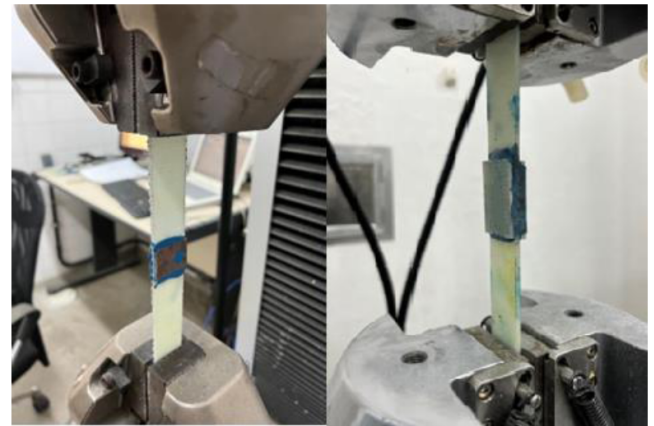
Figure 12: Tensile tests with carbon steel and GFRP patches.

For holes with 3 mm and 6 mm diameter, the higher results for carbon steel were patches with 20 mm of
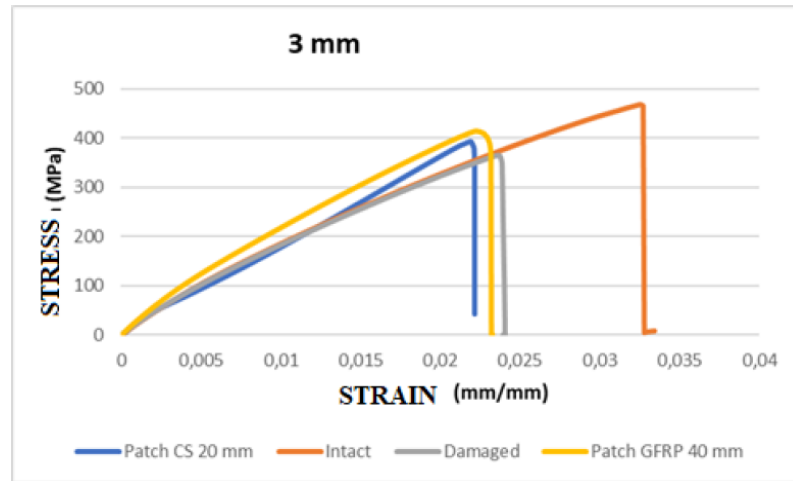
Figure 13: Stress vs strain curves for specimens with a 3 mm hole.
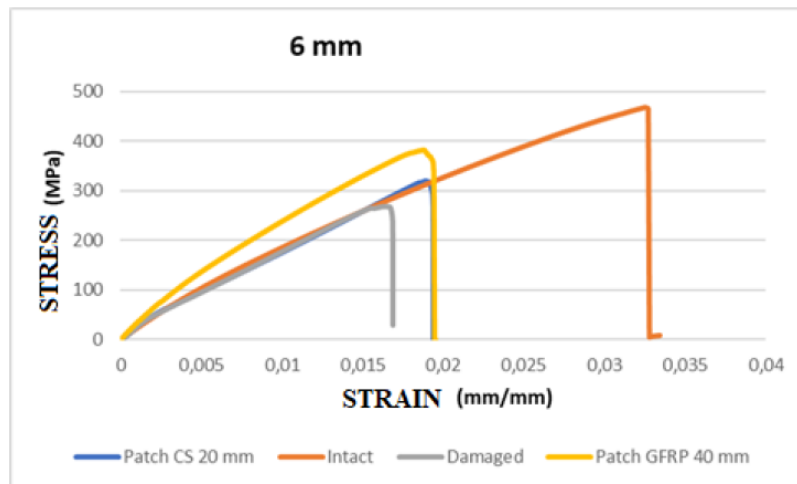
Figure 14: Stress vs strain curves for specimens with a 6 mm hole.
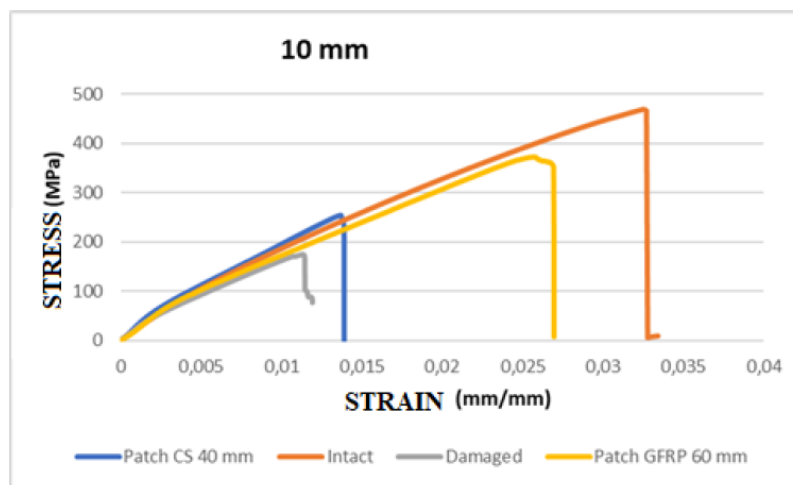
Figure 15: Stress vs strain curves for specimens with a 10 mm hole.

length. For hole with 10 mm, the higher result was patch with 40 mm of length. The results of carbon steel patches were inferior to GFRP patches.

As expected, the highest concentrations were around the 10 mm hole. Layer delamination, fiber breakage and matrix fracture were detected after the
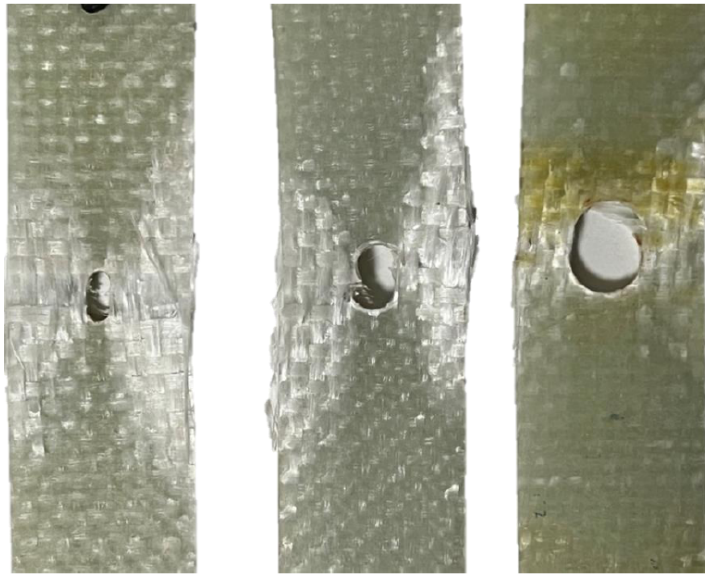
Figure 16: Specimens after Tensile Tests.

conclusion of the tests. In Figure **15**, a photo of the damaged test specimens is shown after carrying out the tests without repair.

The specimens were illuminated with a flashlight before the tests and afterwards to visually check the presence of delamination, fiber breaks, lack of resins and impurities in the intermediate layers. Below are photos in Figure **16** of these records.

There are only records of delamination, fiber breaks and matrix fractures after tensile tests. Two different directions for crack propagation were observed. In Figure **17**, the first configuration. In these cases, less delamination and fewer broken fibers were observed.

In Figure **19**, the second configuration. In these cases, it was observed that the delamination was longer, and the fibers broke much more. Some specimens even broke completely.

Although it is not the goal of the present study, it is interesting to make some remarks about the stress distribution and failure criteria. Figure **19** shows an orthotropic plate with a circular hole under traction. x_1 and x_2 are the fiber directions. The hole diameter is noted R. The laminate stress along fiber direction is usually noted $\sigma_{11}(x_1, x_2)$. The laminate stress
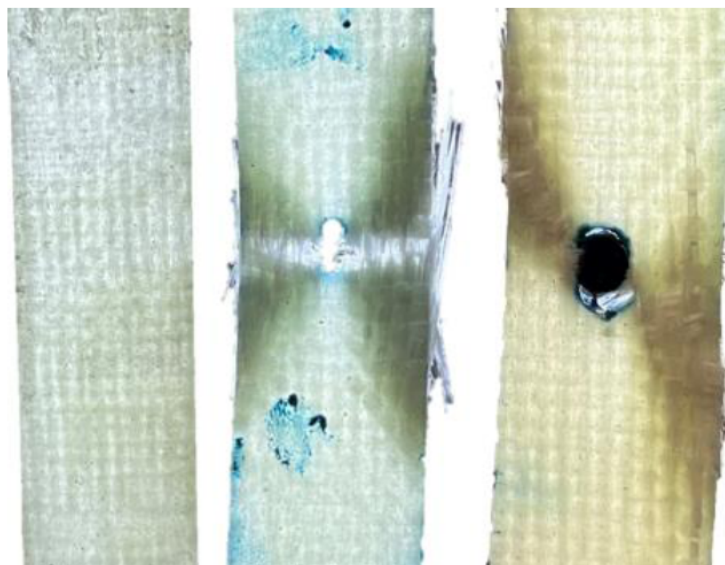
Figure 17: Specimens Illuminated with a Flashlight.
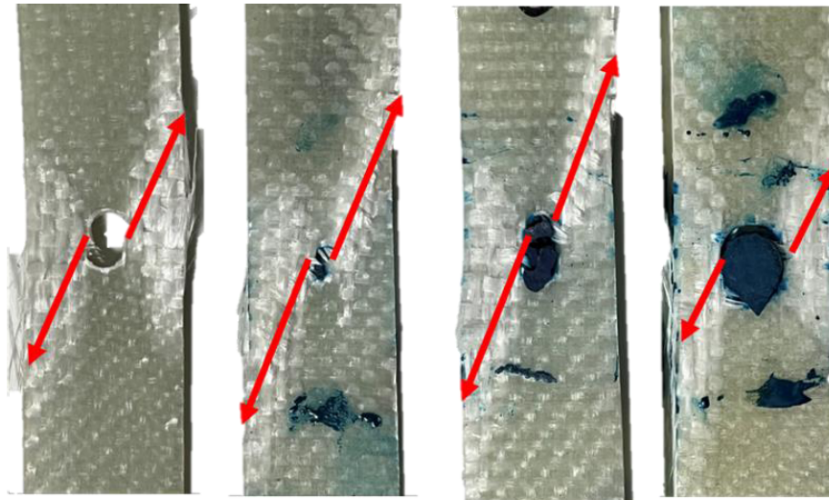
Figure 18: Type I Crack Propagation Direction.
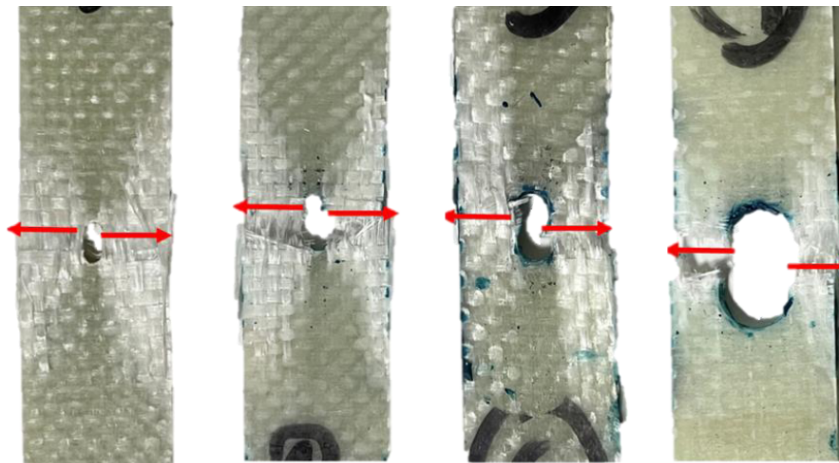
Figure 19: Type II Crack Propagation Direction.

transverse to fiber direction is usually noted $\sigma_{22}(x_1,x_2)$ and the laminate shear stress is usually noted $\sigma_{12}(x_1,x_2)$.
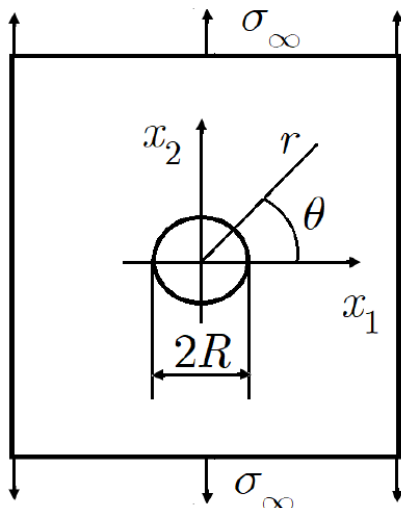
Figure 20: Tensile test of an orthotropic plate with a circular hole.

Eventually it is more interesting to express the stress tensor components in polar coordinates: $\sigma_{\theta\theta}(r,\theta)$, $\sigma_{r\theta}(r,\theta)$ and $\sigma_{rr}(r,\theta)$. A classical boundary condition implies that the forces applied on the boundary of the hole must be equal to the product between the stress tensor and the unit outward normal vector. Since there are no external forces acting on the external surface of the hole, it comes that

$$\begin{bmatrix} \sigma_{rr}(r=R,\theta) & \sigma_{r\theta}(r=R,\theta) \\ \sigma_{\theta r}(r=R,\theta) & \sigma_{\theta\theta}(r=R,\theta) \end{bmatrix} \begin{pmatrix} -1 \\ 0 \end{pmatrix} = \begin{pmatrix} 0 \\ 0 \end{pmatrix} \Rightarrow$$

$$\sigma_{rr}(r=R,\theta) = \sigma_{\theta r}(r=R,\theta) = 0$$

(1)

Thus, the only possible nonzero stress component in polar coordinates is $\sigma_{\theta\theta}(r=R,\theta)$. In this sense, the state of stress in polar coordinates for $(r=R)$ is always unidimensional. The maximum of this tangential stress component depends on the angle θ. Generally, it is maximum for $\theta=0$ and $\theta=\pi$.

$$\sigma_{\theta\theta}(r = R, \theta = 0) = \sigma_{\theta\theta}(r = R, \theta = \pi) = K_T \sigma_\infty \quad (2)$$

where K_T is called the stress intensity factor that can be obtained in tables. This problem has been studied analytically for a long time, for instance by Green and Zerna [23] and Lekhnitskii [24]. Although the plate with a hole under traction with a bonded patch is not the same problem, it is reasonable to search for a phenomenological failure criterion for orthotropic plates with the following form

$$\sigma_{\theta\theta}(r = R, \theta) < \sigma_{\max}(\theta) \quad (3)$$

where $\sigma_{\max}(\theta)$ varies with θ. It is possible to obtain expressions for $\sigma_{\max}(\theta)$ using criteria similar to the Tsai–Wu failure criterion [24] and tensile tests in different directions. The value $\sigma_{\max}(\theta)$ decreases from $\theta = 0$ to $\theta = \pi/2$ what could explain that failure (fracture, delamination, etc) may occur for values of q different than $0 = \pi$. This study will be presented in a forthcoming paper.

CONCLUSION

Visual inspections carried out before and after drilling did not identify delamination between the layers, broken fibers, disoriented fibers, or lack of resin in the surface layers. The fractures were caused by the breakage of the fibers and cracks in the matrix. The failures occurred simultaneously with the sudden detachment of the patches. The repair efficiency directly depends on adhesion at the interface between the adhesive and the repaired material. Holes reduce the useful area of the specimen that resists loading and generate stress concentrations at the edges of the holes. As expected, the larger the hole, the greater the area reduction and the lower stress concentration factor.

The results with GFRP patches were superior to carbon steel patches. Therefore, the recommendation of this dissertation is for 3 mm and 6 mm holes to use GFRP patches with 40 mm length. For 10 mm holes, use GFRP patches with 60 mm. These results were due to the established methodology for manufacturing the specimens and selection of the adhesive that provided high adhesion between the specimens and the patches.

The experimental results were significant for a relatively small sample of tensile tests. For studies with a larger number of tests, non-destructive testing of the specimens must be considered before carrying out the tests. Thermography is cheaper and easier to perform

than ultrasound and radiography. The infrared radiation emitted from each object varies with temperature, which allows changes in temperature to be measured by the infrared camera allowing the depth, size, and location of delamination to be assessed. Further studies shall verify the necessity to analyze the microstructure around the hole before and after the tensile test.

This type of repair is not yet a qualified technique. As the results achieved were very promising, the next studies should be dedicated to certification and approval of the repair technique. Also, a review shall be issued to compare the technique results with other types of repairs.

REFERENCES

[1] da Costa-Mattos HS, Reis JML, Sampaio RF, Perrut VA. An alternative methodology to repair localized corrosion damage in metallic pipelines with epoxy resins. Mater Des 2009; 30: 3581-91.
https://doi.org/10.1016/j.matdes.2009.02.026

[2] Shamsuddoha MD, Mainul Islam MD, Aravinthan T, Manalo A, Lau K. Effectiveness of using fibre-reinforced polymer composites for underwater steel pipeline repairs. Compos Struc 2013; 100: 40-54.
https://doi.org/10.1016/j.compstruct.2012.12.019

[3] da Costa Mattos HS, Reis JML, Paim LM, as Silva ML, Amorim FC, Perrut VA. Analysis of a glass fibre reinforced polyurethane composite repair system for corroded pipelines at elevated temperatures. Compos Struc 2014; 114: 117-123.
https://doi.org/10.1016/j.compstruct.2014.04.015

[4] Alabtah FG, Mahdi E, Eliyan FF. The use of fiber reinforced polymeric composites in pipelines: A review. Compos Struc 2021; 273: 114595.
https://doi.org/10.1016/j.compstruct.2021.114595

[5] Freitas Rachid FB, Costa Mattos HS. Modelling of pipeline integrity taking into account the fluid-structure interaction. International Journal for Numerical Methods in Fluids 1998; 28(2): 337-355.
https://doi.org/10.1002/(SICI)1097-0363(19980815)28:2<337::AID-FLD724>3.0.CO;2-6

[6] da Silva ML, da Costa Mattos H. Failure pressure estimations for corroded pipelines. Materials Science Forum 2013; 758: 65-76.
https://doi.org/10.4028/www.scientific.net/MSF.758.65

[7] da Costa Mattos HS, Reis JML, Paim LM, da Silva ML, Lopes Junior R, Perrut VA. Failure analysis of corroded pipelines reinforced with composite repair systems. Compos Struc 2016; 59: 223-236.
https://doi.org/10.1016/j.engfailanal.2015.10.007

[8] Budhe S, Banea MD, Rohem NRF, Sampaio EM, de Barros S. Failure pressure analysis of composite repair system for wall loss defect of metallic pipelines. Compos Struc 2017; 176: 1013-1019.
https://doi.org/10.1016/j.compstruct.2017.06.044

[9] Mahdi E, Eltai E. Development of cost-effective composite repair system for oil/gas pipelines. Compos Struc 2018; 202: 802-806.
https://doi.org/10.1016/j.compstruct.2018.04.025

[10] Watanabe Junior MM, Reis JML, da Costa Mattos HS. Polymer-based composite repair system for severely corroded circumferential welds in steel pipes. Eng Failure

Analysis 2017; 81: 135-144.
https://doi.org/10.1016/j.engfailanal.2017.08.001

[11]   da Costa Mattos HS, Reis JML, Amorim FC, Brandao JFS, Lana LDM, Perrut VA. Long-term field performance of a composite pipe repair under constant hydrostatic pressure. Eng. Failure Analysis 2021; 130: 105765.
https://doi.org/10.1016/j.engfailanal.2021.105765

[12]   Sathler JF, de Luca CR, Reis JML, da Costa Mattos HS. Alternative methods for fracture energy acquisition in the qualification of composite repair system. compos structures 2021; 258: 113420
https://doi.org/10.1016/j.compstruct.2020.113420

[13]   De Luca CR, Reis JML, Mota GP, da Costa Mattos HS. Addition of silica in the adhesive primer layer of composite systems used to repair leak defects in metallic pipelines. Composite Structures 2023; 321: 117289
https://doi.org/10.1016/j.compstruct.2023.117289

[14]   ASME PCC-2. Repair of pressure equipment and piping, 2022. https: //www.asme.org/codes-standards/find-codes-standards/pcc-2-repair-pressure-equipment-piping

[15]   ISO Technical Specification 24817. Petroleum, petrochemical and natural gas industries. Composite repairs for pipework. Qualification and design, installation, testing and inspection, 2015. https: //www.iso.org/standard/59987.html

[16]   Reis JML, Costa AR, da Costa Mattos HS. Repair of damage in pipes using bonded GFRP patches. Com João Laredo dos Reis e Alexander Rodrigues Costa. Composite Structures 2022; 296: 115875
https://doi.org/10.1016/j.compstruct.2022.115875

[17]   Miranda BM, Reis JML, da Costa Mattos HS. Analysis of the adhesive thickness effect on failure pressure of metal/composite hybrid joints in pressurized blister tests. Com Miranda, B.M., Reis, J.M.L., International Journal of Adhesion and Adhesives 2023; 121: 103314.
https://doi.org/10.1016/j.ijadhadh.2022.103314

[18]   Baker A. Bonded composite repair of fatigue-cracked primary aircraft structure. Composite Structures 1999; 47: 431-443
https://doi.org/10.1016/S0263-8223(00)00011-8

[19]   Zhenhui Sun, Cheng Li, Ying Tie. Experimental and numerical investigations on damage accumulation and energy dissipation of patch-repaired CFRP laminates under repeated impacts. Materials & Design 2021; 202: 109540
https://doi.org/10.1016/j.matdes.2021.109540

[20]   FU, Yutong; Yao, Xuefeng; A Review on Manufacturing Defects and Their Detection of Fiber Reinforced Resin Matrix Composites. Composites Part C: Open Access 8 (2022) 100276.
https://doi.org/10.1016/j.jcomc.2022.100276

[21]   ASTM D3039/D3039M-08 Standard Test Method for Tensile Properties of Polymer Matrix Composite Materials. 2014

[22]   Oliveira MJ, Enne FF, Reis JML, da Costa Mattos HS. Alternative surface treatments for the repair of through-wall corrosion damage in metallic pipes with bonded plates, The Journal of Adhesion 2022; 98(16): 2643-2661
https://doi.org/10.1080/00218464.2021.1986395

[23]   Green AE, Zerna W. Theoretical Elasticity, London, U, K: Clarendon Press, 1954.

[24]   Lekhnitskii G. Anisotropic Plates, translated from the second Russian edition bay, S.W, Tsai and T, Cheron, Gordon. Breach Science Publishers Inc, N4. 3, 1968.

[25]   Gay D, Hoa SV, Tsai. SW. Composite Materials. Design and Applications. 1st Edition, CRC Press, Boca Raton, 2002.
https://doi.org/10.1201/9781420031683